CARBON 46 (2008) 1860–1868

available at www.sciencedirect.com

ScienceDirect

journal homepage: www.elsevier.com/locate/carbon

The confined growth of double-walled carbon nanotubes in porous catalysts by chemical vapor deposition

Yi Liu, Wei-zhong Qian*, Qiang Zhang, Guo-qing Ning, Qian Wen, Guo-hua Luo, Fei Wei

Beijing Key Laboratory of Green Chemical Reaction Engineering and Technology, Department of Chemical Engineering, Tsinghua University, Beijing 100084, China

ARTICLE INFO

Article history:
Received 9 May 2007
Accepted 25 July 2008
Available online 11 August 2008

ABSTRACT

Double-walled carbon nanotubes (DWCNTs) were prepared from methane using a Fe/MgO porous catalyst. A series of catalyst powders with different pore size distributions were obtained by compression at pressures of 0–233 MPa. These were used to decompose methane and synthesize DWCNTs which differed in activity, purity, yield and degree of perfection. Characterization by transmission electron microscopy, scanning electron microscopy, Raman spectroscopy, thermo-gravimetric analysis, N_2 adsorption measurement (Brunauer–Emmett–Teller (BET)) and Hg penetration provided direct evidence that a compact catalyst structure is not good for the nucleation and growth of DWCNTs, e.g., a catalyst with a compact structure that did not have pores larger than 30–50 nm mostly produced multi-walled carbon nanotubes. The confined growth and buckling model of DWCNTs inside the porous catalysts are proposed to explain the growth behavior. These results suggest that a porous catalyst for DWCNT synthesis should have a large pore size distribution or loose stacked structure, which provides new guidelines for catalyst design.

1. Introduction

Composed of two coaxial single-walled carbon nanotubes (SWCNTs), double-walled carbon nanotubes (DWCNTs) integrate the excellent mechanical and electrical properties of SWCNTs and the chemical and thermal stability of multi-walled carbon nanotubes (MWCNTs). DWCNTs would find application in field emission devices [1] and super-tough fibers [2–4]. In the chemical vapor deposition (CVD) process to prepare DWCNTs, active components are usually deposited on porous supports, such as Al_2O_3, MgO, SiO_2, etc. [5–18], which is one of the most important processes due to easy mass production at low cost. Major focus has been put on keeping a high specific surface area (SSA, Brunauer–Emmett–Teller (BET)) and dispersing the metal nanoparticles (NPs) on the catalyst to control the nucleation [10,13], so as to control the purity and yield of DWCNTs. However, the resistance during the growth, in the scale of sub-micrometer, has been concerned rarely. It is noted that the contribution to the SSA of porous catalysts mainly comes from the existence of micropores (<2 nm) and mesopores (2–50 nm) [19]. Apparently, due to their small size, these pores would not be large enough to hold DWCNT products, which are usually several to several tens micrometers long, unless the catalyst structure is destroyed. Thus it can be suggested that the pore structure of the catalyst can have a negative effect on the growth of DWCNTs. An understanding of this process will help us find novel ways to design catalysts to prepare DWCNTs with much higher yields and better quality.

In order to address this problem quantitatively, we studied the effect of the catalyst structure on the DWCNT growth using a model Fe/MgO catalyst [17] compressed at different pressures (0–233 MPa). Catalyst powders with the same chemical properties (composition, metal loading and size), but

* *Corresponding author:* Fax: +86 10 62772051.
E-mail address: qwz@flotu.org (W.-z. Qian).
0008-6223/$ - see front matter
doi:10.1016/j.carbon.2008.07.040

different physical properties (pore size distribution, hardness, density and BET SSA) were obtained. Thus, when DWCNTs were prepared on these catalysts with the same CVD process, the relationship between these physical properties of the catalyst powders and the products (yield, degree of perfection, SSA) can be obtained. Notably, we found that the yield, purity, quality and morphology of the carbon products were significantly affected by the pore size or hardness of the catalyst agglomerate, rather than its BET SSA. Specifically, the dominant carbon products were changed from DWCNTs to carbon capsules/MWCNTs when the pressure exerted on the catalyst powder was higher than 56 MPa. A buckling model was used to explain the confined growth process of DWCNTs inside the porous catalysts.

2. Experimental

A model Fe/MgO catalyst with Fe loading of 3 mol% was prepared by the impregnating method and hydrothermal treatment, reported elsewhere [17]. The catalysts are not spherical particles but small sheets with size of 100–500 nm and thickness of 10–30 nm (Fig. 1a). The agglomerates of these sheets are several micrometers in diameter (see Supplementary Information, Fig. S1). After calcination at 873 K for 2 h, many holes smaller than ~60 nm appeared on the sheets due to the dehydration of $Mg(OH)_2$ (Fig. 1b). Five to ten grams catalyst powder was filled into a cylindrical container with an inner diameter of 3 cm. Then cold pressing was carried out vertically on the catalyst powder at different pressures (see Supplementary Information, Fig. S2). No lubricant was used in the experiment to avoid the pollution of the samples.

The compressed catalyst cake was crushed to a powder of ~50 μm in size. 20 mg catalyst powder was put into a quartz tube reactor [17,18] and heated to 1023 K in Ar (99.999% purity) atmosphere. Then the mixed gases of Ar and CH_4 (99.99% purity) (with a volume ratio of 1:1 and a total flow rate of 20 ml/min) were fed into the reactor. CH_4 was decomposed by the catalyst to grow DWCNTs for 15 min. The product gas was analyzed by an online gas chromatography (Shimadzu 14B). Thus, the conversion of CH_4 was obtained. The thermal decomposition of CH_4 is not serious at 1023 K, so the formation of nanotube or amorphous carbon is mostly attributed to the properties of the catalyst.

The pore size distribution of catalysts after calcination was measured by an ex-situ Hg penetration method. The BET SSA of the catalyst and products were measured online by a single point BET SSA measurement system placed in the reaction system [18]. The crystallite size of catalyst support was characterized by a X-ray diffraction (XRD, O8-DISCOVER diffractometer, nickel-filtered Cu K_α radiation target) and calculated by Scherrer equation based on the (220) crystallite. Carbon products grown on catalysts compressed at different pressures were characterized by high resolution transmission electron microscopy (HRTEM, JEOL 2010F, 200.0 kV), scanning electron microscopy (SEM, JSM 7401F, 1.0 kV), Raman spectroscopy (Renishaw, RM2000, He–Ne laser excitation line at 633 nm) and thermo-gravimetric analysis (TGA, TA-2050).

3. Results and discussion

Monitoring the pore size distribution of the catalyst powder showed clearly the evolution of the pores with pressing pressures (Fig. 2a). There are three-hierarchical pores in the original catalyst powder with a wide pore size distribution ranging from 10 nm to 5 μm. The pores smaller than ~60 nm and larger than ~1 μm are ascribed to the holes in the catalyst sheets (Fig. 1b) and the cavities between the catalyst agglomerates, respectively. The pores of 0.1–1 μm are the interspaces between the randomly stacked catalyst sheets in agglomerates, which are mostly concerned in this article. After the compression at 5.6, 28, and 56 MPa, respectively, pores larger than 600, 200 and 60 nm disappeared with the dominant pore size of the agglomerates decreased from about 110 to 36 nm gradually. With the gradual increase in the pressure exerted, multi peaks merged into one peak, and the pores larger than 60 nm (correspond to the interspaces between catalyst sheets) disappeared, especially there was a jut in the range 20–30 nm for the sample compressed at 56 MPa, indicating the agglomerates were crushed (Fig. S3) and the interspaces between catalyst sheets were eliminated completely followed by an

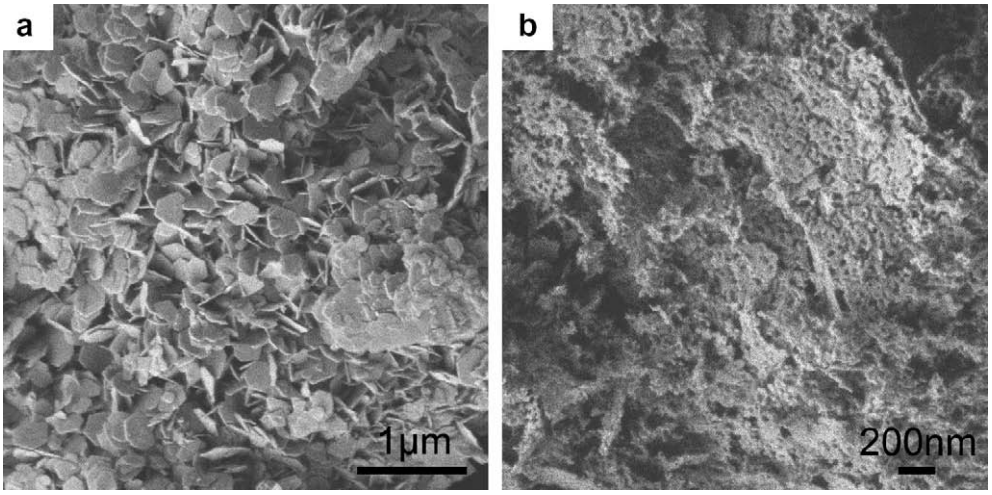

Fig. 1 – SEM morphologies of catalyst: (a) catalyst precursor, and (b) after calcination at 873 K.

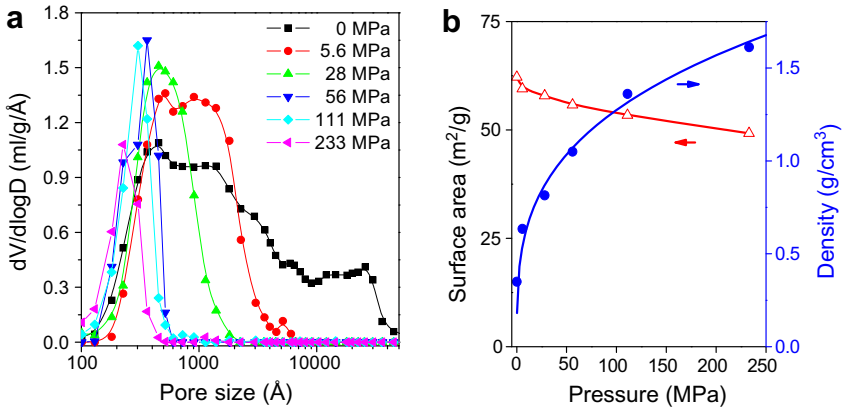

Fig. 2 – Characterization of catalyst powder compressed at different pressures: (a) pore size distributions, and (b) the SSA and grain densities.

increase of pores smaller than 30 nm. On further increasing the pressing pressure to 233 MPa, the dominant pore size kept on dropping down to ~20 nm, and the peak value decreased, however the changes slowed down.

With the loss of pores larger than 60 nm, the catalyst agglomerate became more compact and the density of the material (after pressure release) increased monotonically with the pressing pressure (Fig. 2b). This tendency is similar to that of the compression of metal powder and other materials. Specifically, the density of the catalyst powder increased from 350 kg/m^3 for the original catalyst to 1500 kg/m^3 for that treated at 233 MPa, which was a 4 fold increase. Comparatively, the BET SSA of the catalyst (calcinated at 1023 K, which is same as the temperature for DWCNT growth; Fig. 2b) only decreased from ~60 m^2/g (the original catalyst) to ~50 m^2/g (compressed at 233 MPa). This change is relatively minor compared with the changes in the pore size distribution and density of the catalyst powder.

These catalysts were then used to decompose CH_4 and make CNTs. Kinetic process of decomposing CH_4 is shown in Fig. 3. The original non-compressed catalyst had a high

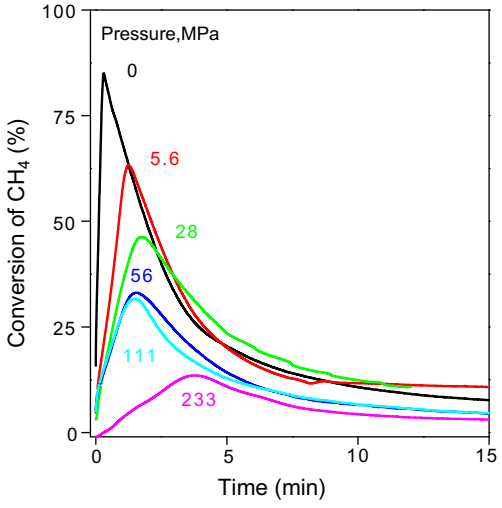

Fig. 3 – Delayed DWCNT growth in the compressed catalyst powder.

activity for decomposing CH_4. The time of the peak position (for the conversion of CH_4) appeared at 0.1 min. It, however, increased up to about 2 min with increasing pressure exerted on the catalyst powder (5.6–111 MPa), an obvious delay. Meanwhile, the peak values also decreased with increasing pressures exerted on the catalyst, indicating the low activity of the compressed catalysts. Specifically, the peak value for the catalyst compressed at 233 MPa decreased to be about one seventh of that for the original catalyst, which was accompanied by a much longer delay for 4.5 min. These results evidenced clearly that the decomposition of CH_4 to form carbon products are significantly hindered by the increasing pressures exerted on the catalyst. Notably, the differences in the negative effect of applied pressure on the catalyst mostly occurred before the appearance of peak value (for the conversion of CH_4). Comparatively, the deactivation tendencies (in the time after the appearance of the peak of methane conversion), mainly due to the sintering of active components and the coke encapsulation effect on the metal NPs [14], were similar for all the catalysts. Considering the chemical composition of the catalysts are all the same, these results suggested that the low activity and the slow DWCNT growth process described above were mainly due to the compression of the catalyst powder, purely a physical effect.

TEM images present the typical morphologies of the carbon products grown on the catalyst powder compressed under different pressures (Fig. 4). When the pressure was lower than 56 MPa, the dominant carbon products were DWCNTs. DWCNTs grown on the non-compressed catalyst had a relatively perfect morphology and were mostly bundled. However, with increasing pressing pressure, some short DWCNTs and broken nanotubes or carbon fragments appeared. Also, the bundle size and the ratio of bundled DWCNTs decreased (see Supplementary Information, Fig. S4 and S5). Even worse, the carbon products from the catalysts compressed above 56 MPa, were not DWCNTs, but were mainly carbon capsules or short MWCNTs. These results had not been reported and indicated an undiscovered effect.

Raman spectra (Fig. 5a) also showed that, with increasing pressures exerted on the catalyst powder, the intensities of the peak of radial breathing modes (RBM, 100–250 cm^{-1}) and the G band (~1590 cm^{-1}) of the carbon products decreased

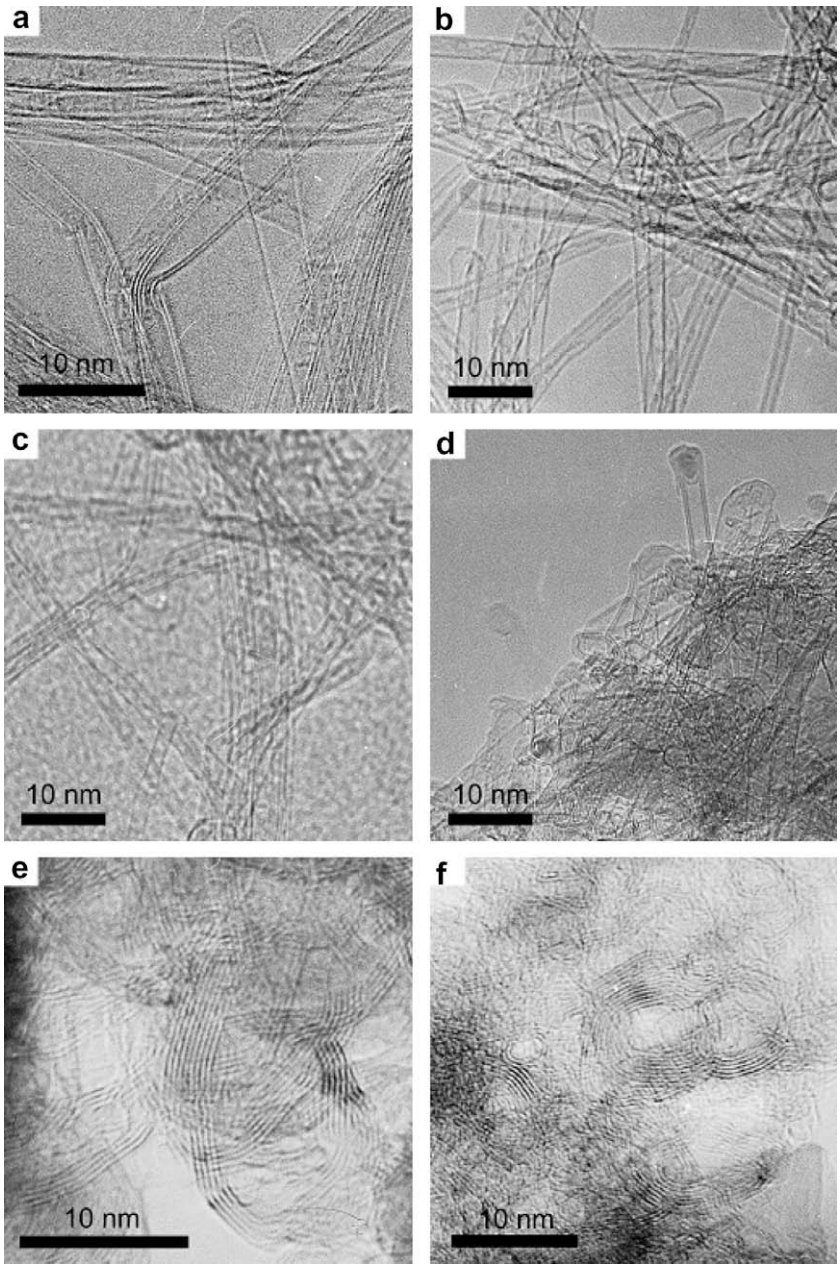

Fig. 4 – TEM images of the carbon products prepared by catalyst powder compressed under different pressures: (a) 0 MPa, (b) 5.6 MPa, (c) 28 MPa, (d) 56 MPa, (e) 111 MPa, and (f) 233 MPa.

significantly. Surprisingly, the RBM peak of the products nearly disappeared when the pressing pressure on the catalyst was above 56 MPa, which also suggested that in this case, the dominant products might not be DWCNTs but were others, e.g. MWCNTs or carbon capsules. Furthermore, when we used the intensity ratio of the D band (~1320 cm^{-1}) to G band (I_D/I_G) to evaluate the degree of perfection of the CNTs, the insert in Fig. 5a shows that I_D/I_G value increased significantly with the pressure exerted on the catalyst powder. The I_D/I_G value of the carbon product at 111–233 MPa was close to 1, which implied that the products were mostly amorphous carbon or MWCNTs.

Meanwhile, BET SSA of carbon products also confirmed that the quality of the products was seriously affected by applied pressure. Fig. 5b shows that the BET SSA of the carbon products decreased with the pore size reduced. The SSA of the carbon product prepared from the original catalyst was around 600 m^2/g, but it was only 171 m^2/g for that prepared from a catalyst compressed at 233 MPa with a dominant pore size of ~20 nm, which was close to those for MWCNTs or carbon black. These results indicated that the content of carbon impurities, such as carbon fragments and MWCNTs, increased in the products from the catalyst compressed at pressures above 56 MPa, in agreement with the TEM observation (Fig. 4).

On further correlating the carbon yield with the pore size of the catalyst powders, it can be seen that powders with different pore sizes gave different increasing carbon yield

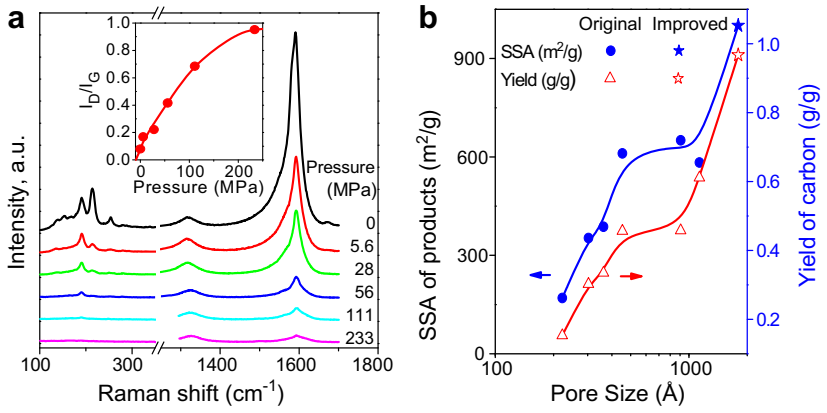

Fig. 5 – Characterization of products prepared by compressed catalyst powder: (a) Raman spectra of products, and (b) relations between the yield, specific surface area of carbon products and the dominant pore size of the catalyst powder. The inset in (a) is the relationship of defects (I_D/I_G value) in the products with the pressing pressures.

(Fig. 5b). The yield was lower than 0.2 g carbon per gram catalyst powder when the powder with a dominant pore size of ~20 nm was used. However, it increased up to about 0.6 gradually for catalyst with a dominant pore size larger than 110 nm. It indicated that the catalyst powder with a large pore size had sufficient space inside and allowed the formation of carbon in high yield.

The results of TEM observation, Raman spectra and BET SSA all gave the evidence that a catalyst with a compact structure not only gave a low yield, but also gave a low quality and/or low content of DWCNTs in the gross product. These findings suggested the confined growth of DWCNTs in the porous catalysts.

To clearly understand this, we proposed the growth model of an individual DWCNT inside the pore of the catalyst (Fig. 6). The nucleation of CNTs could be considered as self-assembly

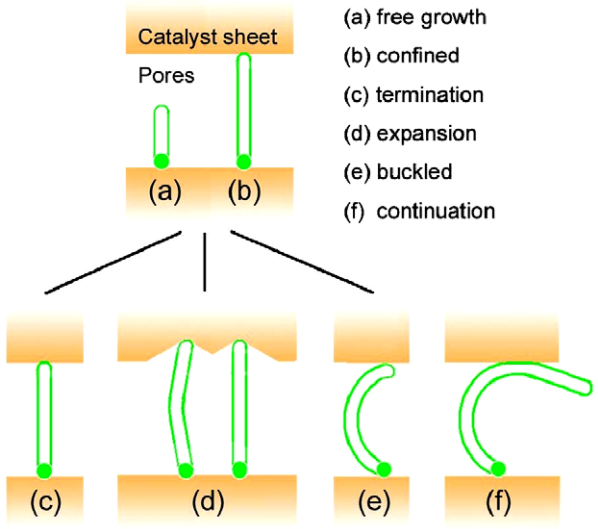

Fig. 6 – Confined growth of an individual DWCNT in a porous catalyst agglomerate: (a) free growth, (b) touching of the catalyst sheet, (c) termination of the growth, (d) pores of catalyst agglomerate broadened, (e) buckled, and (f) continued growth.

of carbon atoms into tubes after precipitating from quasi-liquid saturated C–Fe solution. No matter the tip growth [20] or the base growth [21] mode dominates the nucleation process of the DWCNT, the grown DWCNT always touches the catalyst sheet, and therefore, three possible scenarios will occur: (1) If the catalyst agglomerate is strong and the DWCNT cannot expand the catalyst agglomerate, growth will terminate (Fig. 6c); (2) the DWCNT can expand the catalyst agglomerate and continue to grow if the strength of the catalyst agglomerate is weak (Fig. 6d); (3) the DWCNT cannot expand the catalyst agglomerate but can buckle when the pore size is large enough, then the DWCNT can extend out from the interspaces between catalyst sheets in agglomerate and continue to grow (Fig. 6e and f).

Mechanical force was calculated according to the buckling of the DWCNT in the interspaces between the catalyst sheets quantitatively. The critical compression stress (σ_{crit}) for Euler buckle of DWCNT can be calculated by the equation $\sigma_{crit} = E(\pi r/L_H)^2$ [22–26], where E denotes the Young's modulus (~1 TPa), r is the nanotube radius (1 nm), and L_H is the half length of the nanotube. Larger stress is needed for DWCNTs buckled in smaller pore. For the catalyst pore with the diameter of 100 nm, the calculated stress is 4 GPa. However, when the catalyst was compressed, i.e. at 233 MPa, the catalyst agglomerate got constricted and the pore size decreased. In such limited space, smaller than 30 nm, the critical compression stress would be more than 40 GPa, which may be too large for DWCNT to grow because large deformation of the quasi-liquid metal NPs might occur at such large pressure (see Supplementary Information, Text 1). Maybe the deformed metal NPs led to the failure of DWCNT growth, while carbon capsule/MWCNT (with the diameter of ~10 nm, in the range of the pore size of the compressed catalyst) appeared after the aggregation of such deformed metal NPs in confined space (Fig. 7a). Similar situation has happened to MWCNT arrays when suffering from applied pressure, resulting in more defects and serpentine morphology [27,28]. The mechanical energy [27] suffered from in confined space may be another factor to terminate the DWCNT growth. However, further investigation is needed. Generally, catalysts with strong structure and smaller pores will produce carbon capsules/

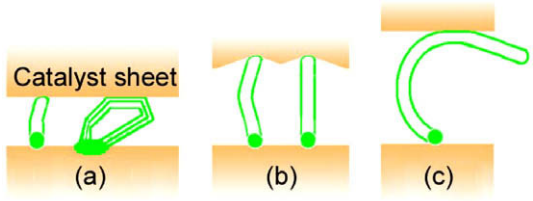

Fig. 7 – Growth modes of CNTs in pores of different sizes: (a) termination of growth or evolution to capsules/MWCNTs in small pore, (b) expanding the medium pores in agglomerate, and (c) buckled and continued growth in large pores.

MWCNTs; Medium pores with weak agglomerate may enable DWCNTs to grow, but accompanied with bad degree of perfection; larger pores make the bulking of DWCNTs possible and growth continued (Fig. 7).

Buckled DWCNTs were indeed found abundantly in the gross product by SEM observation (Fig. 8a). The sheet-like catalyst was kept without obvious break. DWCNT fibers extend in the interspaces between the sheets. Most of them buckled and coiled together. Statistics of about 200 coiled DWCNTs show that the diameter of coils is mostly larger than 200 nm (Fig. 8b), which may be the critical dimension for buckling.

The evolution of crystallite size and pore structure after the DWCNT growth was also studied (Fig. 8c and d). The crystallite sizes of catalysts are all around ~20 nm, however they increased after DWCNT growth, which may be due to the sintering of MgO crystallites. The crystallite size increased much more after DWCNT growth for more compact catalyst (e.g. compressed at 233 MPa). So we can conclude that DWCNTs are unable to crack the MgO crystallite, different from the effect of chemical bond force to destroy the MgO crystallite by lattice mismatch during reaction with CO_2 [16].

The volume of pores smaller than 35 nm increased significantly after the DWCNT growth, indicating that the very short DWCNTs may have a certain possibility to broaden the pores of the catalyst, similar to that of MWCNTs [29]. However, DWCNTs of 100–475 nm in length may buckle in the catalyst agglomerate and occupied the interspaces between catalyst sheets, leading to the reduction of the pore volume, which is in agreement with above calculation and the results of the compaction response (see Supplementary Information, Fig. S3). As to the pores between 500 and 7000 nm (the cavities between agglomerates), they increased significantly (Fig. 8d), maybe due to the weak interaction (e.g. static electrical force or Van der Waals force) between the catalyst agglomerates.

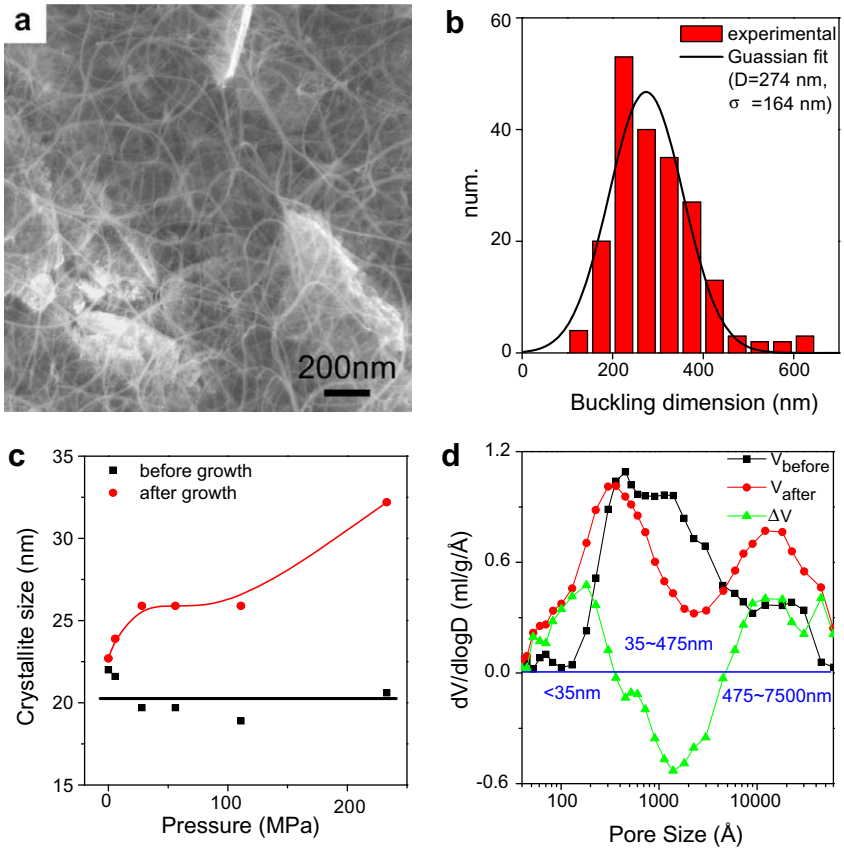

Fig. 8 – Characterization of products and catalysts before and after DWCNT growth: (a) buckled and coiled DWCNTs in the interspaces between catalyst sheets, (b) diameter distribution of the coils, (c) XRD crystallite size of catalyst support, and (d) pore size distribution of non-compressed catalyst. The pore size distribution after DWCNT growth is corrected by dividing by the weight percentage of the catalyst, e.g., if the content of DWCNTs is 30%, then the pore volume is corrected by dividing by 0.70.

The growth of DWCNTs was also compared using different kinds of catalysts (not compressed). Fig. 9a presents an improved catalyst with a larger sheet than the original catalyst in the present work, whose dominant pore size is larger than 180 nm (also see Supplementary Information, Fig. S6). A mixture of DWCNTs and SWCNTs grown on this catalyst has a high carbon yield and a high BET SSA of 1005 m^2/g (Fig. 5b and Table 1), about 1.7 times that grown on the original catalyst (~600 m^2/g). There are abundant DWCNT fibers in the interspaces between the catalyst sheets (Fig. 9b). Comparatively, as using a granulated catalyst, sparse fibers were found in the pores for large granulated catalyst (100–200 nm, Fig. 9c). However, DWCNTs mostly grew on the surface of the agglomerate of small granulated catalyst (20–30 nm, Fig. 9d). Apparently, the different topologies of DWCNTs in the pores or on the surface of catalyst agglomerate are ascribed to the different architectures of the catalyst. Sheet-like catalysts have large interspaces between different sheets, which do not hinder the free growth of DWCNTs in the holes or on the surface of thin catalyst sheet. Thus the journey (equals to the thickness of sheets, ~20 nm) is shortened for DWCNTs growing from the small pore (where nucleation occurred) to large pore (where buckled and growth continued), consequently, the steric hindrance is significantly reduced, compared with that of granulated catalyst where small pores are mainly inside its core. Hence SWCNTs/DWCNTs with a high quality and a high yield were obtained as using sheet-like catalysts.

This work shows the evidence that DWCNT growth not only needs a good dispersion of the active metal components on the catalyst support and a suitable large BET SSA, but also needs a proper catalyst structure (most pores larger than 60 nm, small primary agglomerate, wide pore size distribution, large pore volume and weak interaction between the catalyst sheets/particles in agglomerates). We can conclude that any factors to enlarge the pore size or reduce the strength of catalyst (including the direct formation of large pores in a catalyst by the assistance of organic compounds/materials, controlled critical drying of the catalyst precursor [10], inhibiting catalyst powder sintering at high temperatures, i.e. fast heating method [15], minimizing catalyst support size [16,30], aerosol catalyst [31], ball-milling or direct spray-drying the catalyst to very fine powders, and so on) would provide a cat-

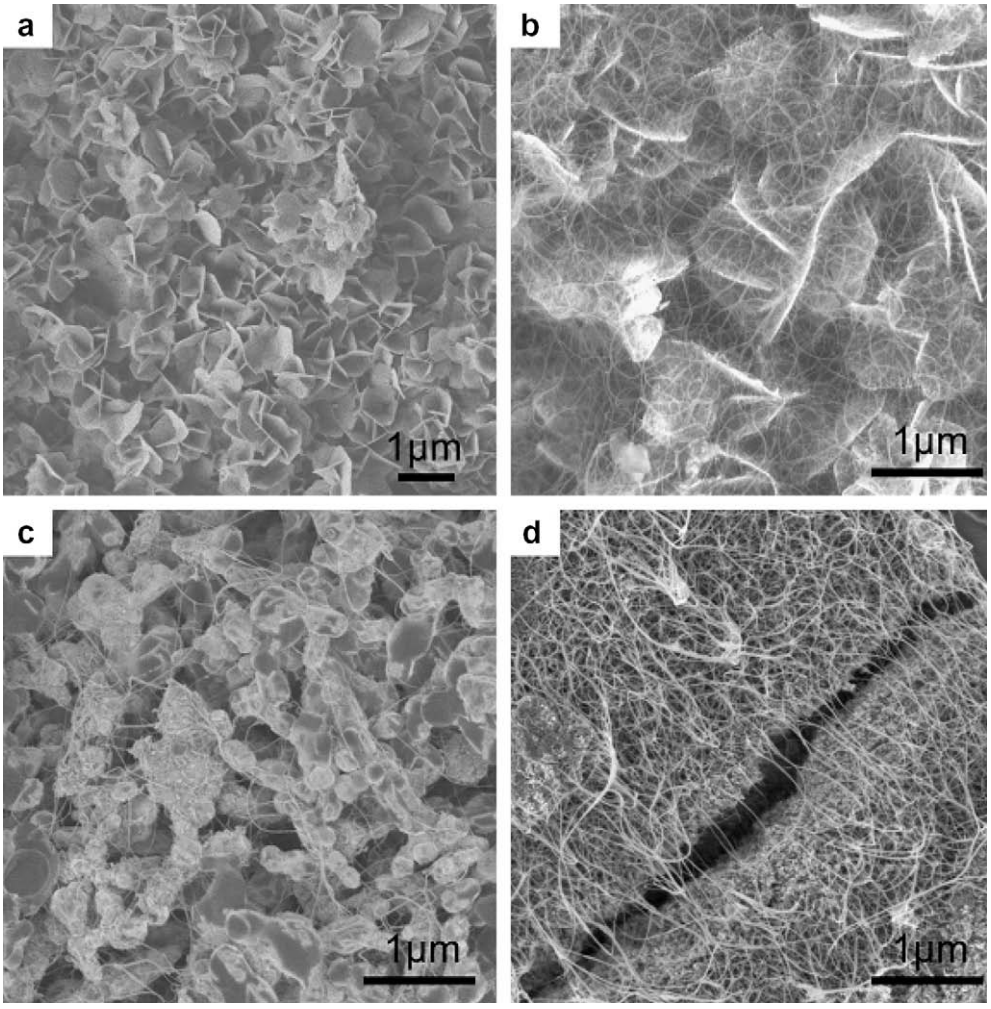

Fig. 9 – Topologies of different catalysts and DWCNTs: (a) SEM images of the improved sheet-like catalysts, (b) as-grown DWCNTs in the improved sheet-like catalysts, and (c, d) DWCNTs grown in the granulated catalyst of different granule sizes. The cajon in (d) was carefully checked by adjusting the focus of microscope, however few DWCNTs were found.

Table 1 – Comparison between original and improved catalysts and their CNT products

Sample	Catalyst		CNT product	
	Sheet size (nm)	Pore size (nm)	Yield (g/g)	SSA (m^2/g)
Original	~300	~110	0.61	~600
Improved	~1000	~180	0.97	1005

alyst with a low bulk density and the weak interaction in agglomerate to meet the requirements of DWCNT growth in high yield, high purity and high quality. These findings provide new guidelines for catalyst design for the preparation of DWCNTs in high purity, high yield and at low cost.

4. Conclusions

Compression of the catalyst powder changes the density, pore size distribution and BET properties of the catalyst powder and this exerts an enhanced confinement effect on the growth of DWCNTs. Consequently, the DWCNT products are obtained in low yield, low purity and with many defects. A buckling model based on a mechanical strength calculation can explain this process well. These findings show that one should give at least the same importance to the pore volume and weak structure of a catalyst as to the BET surface area and dispersion of metal components on the support when a powder is considered for DWCNT synthesis. The findings indicate a conceptually novel method to design a catalyst with relatively weak structure and large pore volume, which is useful for the controlled synthesis of DWCNTs.

Acknowledgements

This work was supported by the National Natural Scientific Foundation of China (Nos. 20606020, 20736004 (key program) and No. 20736007 (key program)), the Foundation of the Author of National Excellent Doctoral Dissertation of PR China (No. 200548), and Chinese national key program (No. 2006CB932702). Key Project of Chinese Ministry of Education (No. 106011). The author was grateful to Prof. Wang Dezheng for the helpful discussions.

Appendix A. Supplementary data

Supplementary data associated with this article can be found, in the online version, at doi:10.1016/j.carbon.2008.07.040.

REFERENCES

[1] Shimada T, Sugai T, Ohno Y, Kishimoto S, Mizutani T, Yoshida H, et al. Double-wall carbon nanotube field-effect transistors: ambipolar transport characteristics. Appl Phys Lett 2004;84(13):2412–4.
[2] Zhang M, Atkinson KR, Baughman RH. Multifunctional carbon nanotube yarns by downsizing an ancient technology. Science 2004;306(5700):1358–61.
[3] Alan BD, Steve C, Edgar M, Joselito MR, Von Howard E, John PF, et al. Super-tough carbon-nanotube fibres. Nature 2003;423(6941):703.
[4] Endo M, Muramatsu H, Hayashi T, Kim YA, Terrones M, Dresselhaus MS. 'Buckypaper' from coaxial nanotubes. Nature 2005;433(7025):476.
[5] Colomer JF, Stephan C, Lefrant S, Van Tendeloo G, Willems I, Konya Z, et al. Large-scale synthesis of single-wall carbon nanotubes by catalytic chemical vapor deposition (CCVD) method. Chem Phys Lett 2000;317(1):83–9.
[6] Flahaut E, Peigney A, Bacsa WS, Bacsa RR, Laurent C. CCVD synthesis of carbon nanotubes from (Mg, Co, Mo)O catalysts: Influence of the proportions of cobalt and molybdenum. J Mater Chem 2004;14(4):646–53.
[7] Lyu SC, Liu BC, Lee SH, Park CY, Kang HK, Yang CW, et al. Large-scale synthesis of high-quality double-walled carbon nanotubes by catalytic decomposition of *n*-Hexane. J Phys Chem B 2004;108(7):2192–4.
[8] Ago H, Nakamura K, Uehara N, Tsuji M. Roles of metal-support Interaction in growth of single- and double-walled carbon nanotubes studied with diameter-controlled iron particles supported on MgO. J Phys Chem B 2004;108(49):18908–15.
[9] Zhu J, Yudasaka M, Iijima S. A catalytic chemical vapor deposition synthesis of double-walled carbon nanotubes over metal catalysts supported on a mesoporous material. Chem Phys Lett 2003;380(5):496–502.
[10] Su M, Zheng B, Liu J. A scalable CVD method for the synthesis of single-walled carbon nanotubes with high catalyst productivity. Chem Phys Lett 2000;322(5):321–6.
[11] Cassel AM, Raymakers JA, Kong J, Dai HJ. Large scale CVD synthesis of single-walled carbon nanotubes. J Phys Chem B 1999;103(31):6484–92.
[12] Geng JF, Singh C, Shephard DS, Shaffer MSP, Johnson BFG, Windle AH. Synthesis of high purity single-walled carbon nanotubes in high yield. Chem Commun 2002(22):2666–7.
[13] Li QW, Yan H, Cheng Y, Zhang J, Liu ZF. A scalable CVD synthesis of high-purity single-walled carbon nanotubes with porous MgO as support material. J Mater Chem 2002;12(4):1179–83.
[14] Yan H, Li QW, Zhang J, Liu ZF. Possible tactics to improve the growth of single-walled carbon nanotubes by chemical vapor deposition. Carbon 2002;40(14):2693–8.
[15] Huang SM, Cai XY, Liu J. Growth of millimeter-long and horizontally aligned single-walled carbon nanotubes on flat substrates. J Am Chem Soc 2003;125(19):5636–7.
[16] Wen Q, Qian WZ, Wei F, Liu Y, Ning GQ, Zhang Q. CO_2-assisted SWCNT growth on porous catalysts. Chem Mater 2007;19(6):1226–30.
[17] Ning GQ, Liu Y, Wei F, Wen Q, Luo GH. Porous and lamella-like Fe/MgO catalysts prepared under hydrothermal conditions for high-yield synthesis of double-walled carbon nanotubes. J Phys Chem C 2007;111(5):1969–75.
[18] Ning GQ, Wei F, Luo GH, Jin Y. Online BET analysis of single-wall carbon nanotube growth and its effect on catalyst reactivation. Carbon 2005;43(7):1439–44.
[19] Hverett DH. IUPAC manual of symbols and terminology for physicochemical quantities and units. Pure Appl Chem 1972;31(4):579–638.

[20] Huang SM, Woodson M, Smalley R, Liu J. Growth mechanism of oriented long single walled carbon nanotubes using "fast-heating" chemical vapor deposition process. Nano Lett 2004;4(6):1025–8.
[21] Li YM, Kim W, Zhang YG, Rolandi M, Wang DW, Dai HJ. Growth of single-walled carbon nanotubes from discrete catalytic nanoparticles of various sizes. J Phys Chem B 2001;105(46):11424–31.
[22] Cao AY, Dickrell PL, Sawyer WG, Ghasemi-Nejhad MN, Ajayan PM. Super-compressible foamlike carbon nanotube films. Science 2005;310(5752):1307–10.
[23] Yakobson BI, Brabec CJ, Bernholc J. Nanomechanics of carbon tubes: Instabilities beyond linear response. Phys Rev Lett 1996;76(14):2511–4.
[24] Waters JF, Guduru PR, Jouzi M, Xu JM, Hanlon T, Suresh S. Shell buckling of individual multiwalled carbon nanotubes using nanoindentation. Appl Phys Lett 2005;87(10):103109.
[25] Li CY, Chou TW. Modeling of elastic buckling of carbon nanotubes by molecular structural mechanics approach. Mech Mater 2004;36(11):1047–55.
[26] Lourie O, Cox DM, Wagner HD. Buckling and collapse of embedded carbon nanotubes. Phys Rev Lett 1998;81(8):1638–41.
[27] Hart AJ, Slocum AH. Force output, control of film structure, and microscale shape transfer by carbon nanotube growth under mechanical pressure. Nano Lett 2006;6(6):1254–60.
[28] Zhang Q, Zhou WP, Qian WZ, Xiang R, Huang JQ, Wang DZ, et al. Synchronous growth of vertically aligned carbon nanotubes with pristine stress in the heterogeneous catalysis process. J Phys Chem C 2007;111(40):14638–43.
[29] Qian WZ, Liu T, Wei F, Wang ZW, Luo GH, Yu H, et al. The evaluation of the gross defects of carbon nanotubes in a continuous CVD process. Carbon 2003;41(13):2613–7.
[30] Zhang Q, Qian WZ, Wen Q, Liu Y, Wang DZ, Wei F. The effect of phase separation in Fe/Mg/Al/O catalysts on the synthesis of DWCNTs from methane. Carbon 2007;45(8):1645–50.
[31] Barreiro A, Kramberger C, Rummeli MH, Grueneis A, Grimm D, Hampel S, et al. Control of the single-wall carbon nanotube mean diameter in sulphur promoted aerosol-assisted chemical vapor deposition. Carbon 2007;45(1):55–61.